

RESEARCH

Open Access



Co-axial electrospaying of injectable multi-cancer drugs nanocapsules with polymer shells for targeting aggressive breast cancers

Mujibur Khan^{1*} , Md. Mahmudul Hasan¹, Anne Barnett¹, Raziye Piranlioglu², Mohammad Rashid², Ahmet Alptekin² and Ali Arbab²

*Correspondence:
mkhan@georgiasouthern.edu

¹ Department of Mechanical Engineering, Georgia Southern University, Statesboro, GA 30458, USA
Full list of author information is available at the end of the article

Abstract

Background: There is growing potential for nanocarrier-based drug delivery in cancer. However, an incomplete understanding of nano–bio interactions and the challenges regarding processing and fabrication in scale-up engineering techniques, controls over drug release, efficacy, and cytotoxicity to the human cell are the major challenges for its clinical success. The purpose of the study was to develop an electrospaying processing of injectable nanonized encapsulated chemotherapeutics to target primary and metastatic breast cancer tumor microenvironment for precise and controlled delivery.

Results: A novel coaxial electrospaying of multiple cancer drugs (paclitaxel and GW2580) as core and polycaprolactam (PCL) as the shell has been developed to produce multi-cancer drug nanocapsules. Using electrospaying process, we have successfully made nanocapsules containing paclitaxel to target breast cancer cells and GW2580, a colony-stimulating factor 1 receptor (CSF1R) inhibitor to target CSF1R+ myeloid cells in the tumor microenvironments (TME). The UV–vis drug release test for 14 days shows a prolonged and sustained release pattern of both the drugs. In vitro and in vivo results showed the effects of nanocapsules containing multiple drugs in controlling the growth of tumor cells and increased survival of the animal bearing breast cancers.

Conclusion: Nanonized multi-cancer drugs were encapsulated in a PCL shell. The drug doses ratio and the polymer-to-drug ratio were controlled by engineered process parameters. The studies showed the importance of making nanocapsules containing nanocrystals of multiple drugs, which will pave the way of making multiple drug combinations in a controlled manner and capsules can be designed for sustained release of the drugs after accumulation into the TME. TME-directed therapy can be a norm in future cancer treatment strategies. These injectable nanocapsules will allow cancer site-specific precision and controlled delivery to cure primary and metastatic breast cancer and to overcome the chemotherapy resistance.

Keywords: Co-axial electrospaying, Injectable nanocapsules, PCL, Paclitaxel, GW2580, Intratumoral administration, In vivo



Introduction

There is growing potential for nanomedicine as effective, safer, and targeted cancer treatment with the recent advancement. However, an incomplete understanding of nano–bio interactions and the challenges regarding processing and fabrication in scale-up engineering techniques, controls over drug release, efficacy, and cytotoxicity to the human cell are the major challenges for its clinical success (Shi et al. 2017). To date, different types of nanoparticles and nanocarriers have been reported. Carbon nanotubes (CNTs) were investigated as nanocarriers where the payload can either be encapsulated in the inner cavity or be attached to the surface. (Eatemadi et al. 2014; Conde et al. 2014; Chen et al. 2017). However, the major drawbacks of CNTs as nanocarriers are their high cytotoxicity, non-biodegradable nature, and poor water solubility. Gold nanoparticles (Au NPs) have also been investigated (Ghosh et al. 2008). Au NPs are mainly prepared using the colloidal synthesis method which has surface plasmon resonance (SPR) bands to convert light into heat and disseminates that heat to kill the cancer cells. However, Au NPs have low colloidal stability in blood flow and high toxicity towards human cell impeding its use as nanocarrier in cancer therapy (Voura et al. 2004). Quantum dots (QD) are fluorescent semiconducting inorganic nanocarriers that have shown potential (Probst et al. 2013). However, the presence of a highly toxic metal component (CdSe, ZnS) in the QD makes it incompatible as a therapeutic agent. Similarly, functionalized superparamagnetic iron oxide nanoparticles (SPIONs) containing magnetite (Fe_3O_4) and maghemite (Fe_2O_3) were also proposed as targeted drug delivery. Although functionalization of SPIONs provides a surface to conjugate drugs and targeting ligands, eventually leads to instantaneous drug release at the specific target (Wahajuddin and Arora 2012). Prolonged and sustained release of drugs is not possible when it is surface conjugated drugs. Furthermore, liposomes, which are lipid bilayer vesicles, are a well-established formulation strategy to improve drug delivery and enhance therapeutic outcomes. Although the application of liposomes has been expanded since its discovery, the advantages have so far been negligible as it has high production cost, short shelf life, and stability, low encapsulation efficacy, rapid clearance from the bloodstream by the reticulo-endothelial system (Sercombe et al. 2015; Yadav et al. 2017).

Biopolymeric nanoparticles have well-known degradation properties which make it easier to controlled/tune drug release patterns with having less to no toxicity due to their biocompatibility. These nanoparticles are reported to be processed by various methods such as nanoprecipitation, nano/micro-emulsification which depends on the polymer, and drug characteristics such as molecular weight, biodegradability, and hydrophobicity, hydrophilicity (Sun et al. 2014). Issues with using polymeric nanoparticles include limited shape and wide size distribution, limited encapsulation efficiency, which eventually affect drug release characteristics (amount, rate, and pathway) (Xu et al. 2013). Moreover, it is extremely difficult to have a scale-up fabrication process of such nanoparticles with controlled doses of drugs and/or multiple drugs (i.e., chemotherapy) if only chemical synthesis processes such as emulsification or nanoprecipitation are followed. For example, to our experience of the micro and nano-emulsification process, most of the drugs we lose during the oil and water solution phase, and the encapsulation efficiency is extremely low to have effective efficacy of the drug (Kumari 2018).

In this study, we have shown a novel engineering fabrication process of coaxial electro-spraying to encapsulate multiple cancer drugs (paclitaxel, GW2580) with polymer (PCL) shells in nanoscale for cancer therapy. In this process, core drug solutions and sheath polymer solution are forced by an electrostatic potential to eject out through different but coaxial capillary channels, resulting in a core-shell structure. The coaxial jet pulsation mode in relation to the solution viscosity, solution miscibility and incompatibility, solution conductivities, molecular weight and spray voltage will lead to a transformative and scalable nanonization and nano-encapsulation of cancer drugs for targeted therapy. The size and morphology of the nanocapsules will also depend on the process parameters, materials characteristics and solution concentrations. In the absence of an applied electric field, distinct phase of droplets (where the polymer solution will engulf the drug solution) will form at the capillary tip under the influence of gravity. With the effect of high voltage, the capillary droplet will atomize into many nanodroplets which eventually are collected as solid nanoparticles. Solution viscosity, electric conductivity and volatility, pumping rate, spinneret to collector distance, etc. will have impact on the resultant formation of drug nanocapsules, and dose control. This engineered process is scalable with higher encapsulation efficiency, prolonged and sustained drug release, size distribution with less than 100 nm, over other techniques due to their versatile control on the engineering process parameters. Drug dose ratios and polymer to total drug ratios are controlled by the solution concentration and solution flow rate through the pump. As coaxial electro-spraying has minimal interaction with drug and polymer solution, it encapsulates the drug into a polymer shell without any further chemical degradation of the drug. Besides, more drug combinational therapy is possible by just adding more solution pumps and its control system.

The nanoscale size of the capsules allows relatively higher intracellular uptake than other nanostructured systems. They can improve the stability of active substances and can be biocompatible with tissue and cells when synthesized from materials such as polycaprolactone (PCL). PCL in biomedical application is suitable for excellent biocompatibility and its ability for longer drug delivery (Woodruff and Hutmacher 2010).

The rationale behind this size range is to utilize the enhanced permeability and retention (EPR) effects of a hypervascular tumor (Mosqueira et al. 2001; Upreti et al. 2013; Aljuffali et al. 2011; Fang et al. 2013). The 10–100 nm nanoparticles utilize this EPR effect to preferentially accumulate and be retained in tumors unlike the free drugs or small molecules that rapidly undergo renal filtration. This phenomenon of the EPR effect has shown that the retention time of drugs packed in nanoparticles is ten times higher than that of free drugs at a tumor site (Li and Wang 2013; Iyer et al. 2006; Prabhakar et al. 2013; Greish 2010). We have successfully processed nanocapsules containing paclitaxel to target breast cancer cells and GW2580, a colony-stimulating factor 1 receptor (CSF1R) inhibitor to target CSF1R+ myeloid cells in the tumor microenvironments (TME). TME comprises tumor cells, myeloid cells, T-cells, stem cells, immune cells, extracellular matrix, blood vessels, etc. There has not been any report on such cancer drug nanonization to target tumor cells and TME, such as tumor-associated macrophages (TAM) or myeloid-derived suppressor cells (MDCs) at the same time. By combining both paclitaxel and drugs that target TME (CSF1R blocker, GW2580), a synergistic therapeutic effect is expected that leads to control of not only the primary breast

tumors, but also the metastatic foci. A few CSF1R blockers are now under clinical trials for different disorders (Butowski et al. 2015; Patwardhan et al. 2014; Smith et al. 2015). The intravenous formulation of both paclitaxel and GW2580 will allow to decrease the total administered dose (significant decrease in toxicity) and increase the bioavailability to the tumors. The nanocapsules can carry as little as 1–5 wt % of the drug when compared to the carrier polymer. Moreover, these nanocapsules containing both drugs can be injected directly into primary tumors at a lower amount and due to sustained release, the effect could be comparable to the IV administered dose with respect to the control of primary tumors.

Experimental (materials and methods)

Synthesis and fabrication method

Polycaprolactone (PCL) of average molecular weight 14 kg/mol was purchased from Sigma-Aldrich and anticancer drug paclitaxel of 98% purity was purchased from AK Scientific. GW2580 (colony-stimulating factor 1 receptor (CSF1R) inhibitor) was procured from LC laboratory (Woburn, MA) and all other chemicals were of reagent grade and purchased from Sigma-Aldrich. Paclitaxel was dissolved in formic acid with a concentration of 4.4 mg/mL. A homogeneous solution was prepared using a magnetic stirrer in a light protective environment. GW-2580 was dissolved in dimethyl sulfoxide (DMSO) with a concentration of 24.34 mg/mL. Both of these solutions were used as core solutions in the electrospaying process. Biocompatible polymer, polycaprolactone (PCL) was dissolved in a combination of three solvents with a concentration of 32.86 mg/mL using a magnetic stirrer. The three-solvent system consists of formic acid (FA), acetic acid (AA) and trifluoroethanol (TFE) with a volume ratio of 9:9:1. The three-solvent system was used to lower the conductivity and volatility of sheath solution compared to core solution. PCL solution was then sonicated for 13–19 h using a vibracell ultrasonic materials processing unit (750-W with 20 kHz). The sonication parameters were: amplitude 30%; pulse frequency: 50 s ON and 10 s OFF; temperature: 47 °C; to avoid the rise of temperature during the sonication process, ice bath of +4 °C was used. A thermocouple was dipped into the solution to measure the temperature with feedback control to maintain the temperature of the solution at around 47 °C.

NF-500 Electrospinning Unit (MECC, Japan) was used for electrospaying the multi-cancer drug nanocapsules. Ultra-coaxial spinneret, a special concentric nozzle was used for core and sheath coaxial stream. Ultrafine coaxial spinneret as shown in Fig. 1, a special concentric nozzle, is used for creating a coaxial stream of two drugs solution in the core and polymer solution at the sheath.

A 27-gauge needle (OD: 0.413 mm) acted as the core nozzle, which was placed concentrically into the shell nozzle (0.8 mm). Solutions were pumped to the spinneret using two separate high-precision syringe pumps and 10 ml NORM-JECT latex-free syringes. For multi-drug encapsulation, a special Y-connector with compatible Luer-lock adaptors was used to have two distinct drug solution flow which goes into the core of the coaxial spinneret. In this case, two separate drug solutions were pumped from two separate syringes. The schematic of the processing technique of the multidrug nanocapsules is shown in Fig. 2a. The electrospaying machine (Fig. 2b) was equipped with two feed pumps at a precise flow rate from 0.2 to 10.0 ml/h. A dehumidifier was attached to

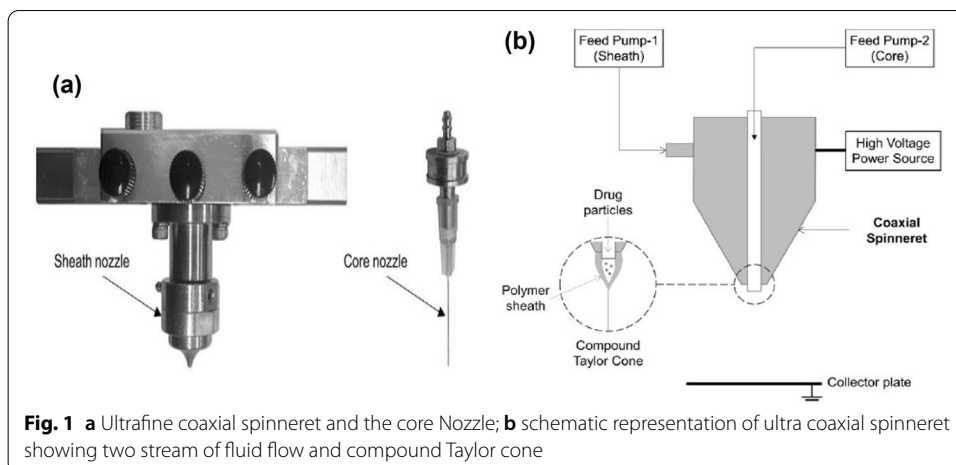


Fig. 1 a Ultrafine coaxial spinneret and the core Nozzle; b schematic representation of ultra coaxial spinneret showing two stream of fluid flow and compound Taylor cone

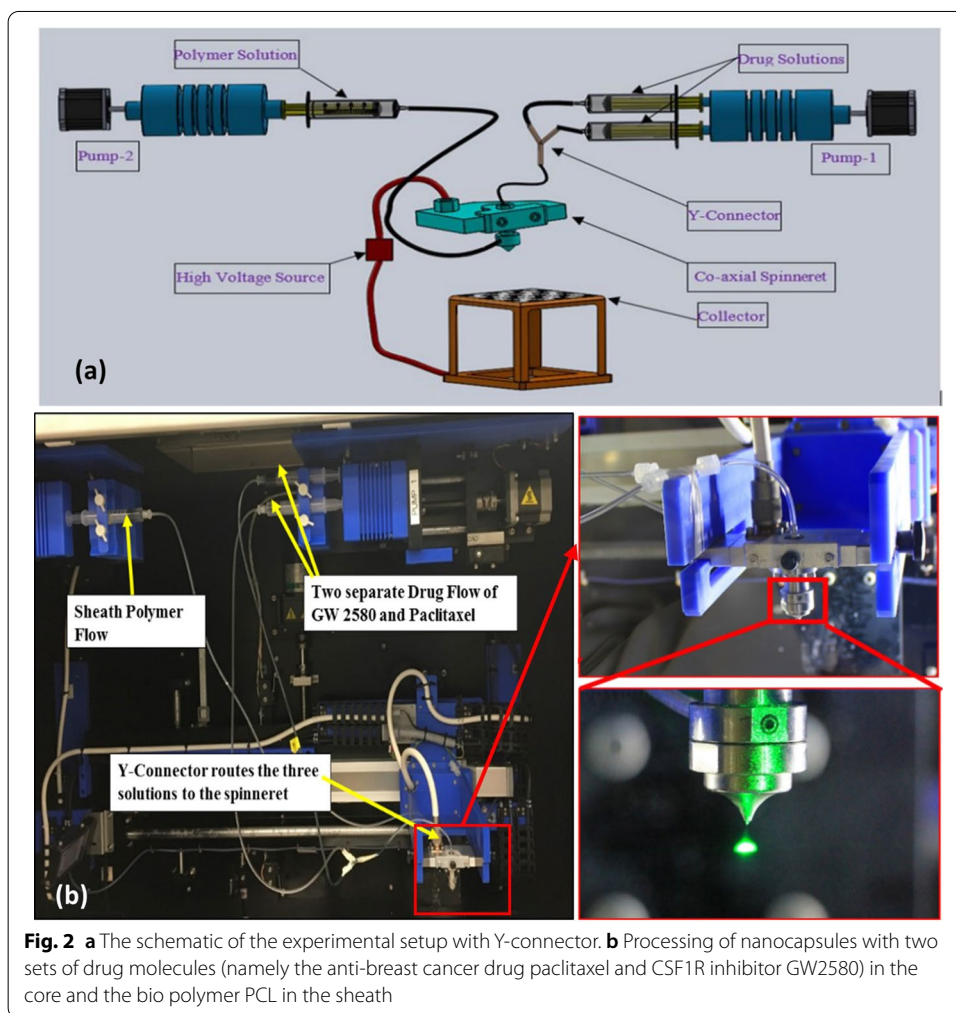


Fig. 2 a The schematic of the experimental setup with Y-connector. b Processing of nanocapsules with two sets of drug molecules (namely the anti-breast cancer drug paclitaxel and CSF1R inhibitor GW2580) in the core and the bio polymer PCL in the sheath

control system humidity. Relative humidity was maintained at around 40% throughout the electro spraying process. The total flow rate (sum of the core and sheath flow rate) was controlled to achieve continuous electro spraying and encapsulation of two drugs

to produce the nanocapsules. The comparative flow ratio and concentration of the two individual drugs were controlled very precisely to maintain the ratio of the mass flow rate according to the doses. The system is capable of processing nanocapsules with multiple drugs with drug weight ratios of 1:1; 1:2; 1:4; 1:8 and more. The weight percentage of the total drugs (paclitaxel + GW2580) was 25% with respect to the polymer sheath, whereas the weight of the paclitaxel-to-GW2580 ratio was maintained at 1:8 in the multidrug nanocapsules. The comparative flow ratio and concentration of the two individual drugs were controlled very precisely to maintain the ratio of the mass flow rate. The system processing parameters (voltage 25–44 kV, tip to collector distance: 140 mm, mass flow rate for paclitaxel solution: 0.1014 $\mu\text{g/s}$; mass flowrate for GW2580 solution: 0.811 $\mu\text{g/s}$; mass flowrate for PCL solution: 2.74 $\mu\text{g/s}$; were kept constant during the processing of the nanocapsules. The nanocapsules were collected in a glass Petri dish kept in the grounded collector surface of the electrospraying machine. The produced nanocapsules were then vacuum dried and weighed. Along with multidrug nanocapsules, single drug nanocapsules of PCL-paclitaxel and PCL-GW2580) were also produced where the drug was in the core and the polymer was in the sheath.

SEM (scanning electron microscope)/TED (transmission electron detector) imaging

SEM and TED images of the as produced nanocapsules were carried out using JEOL 7600 field emission scanning electron microscope (FESEM) with a TED attached to it was used to study the morphology of the particles for the imaging. The TED detector was operated at 30 kV and 2×10^{-4} Torr in order to produce a transmission electron image. Energy dispersive spectroscopy (EDS) was used to investigate the presence of any free drug compound at the outside of the sample. The acceleration voltage was needed to be as high as 20 kV for EDS.

Dynamic light scattering (DLS) assay for size and zeta potential

Size and zeta potential of the nanocapsules containing both drugs were measured by ZetaView Nanoparticle Tracking Analyzer (NTA) system. Nanocapsules were scrapped from the petri dishes and dissolved in distilled water, and dispersed by ultrasonic force. Then, nanocapsules were mixed with PBS (19/1 ratio), and 1 ml of sample was loaded into Zetaview NTA. Nanoparticle size was determined by tracking their Brownian movement in 11 positions and the measurement's statistical average is taken for size evaluation. Zeta potential was measured in 11 measuring positions and two stationary layers with the following parameters; 520 nm laser wavelength, 3.30 V/cm (pulsed) sensed electrical field, and 25 °C temperature. Results were analyzed in ZetaVIEW software (version 8.05.12 SP2) using maximum pixel 200 and minimum pixel 5 and Camera 0.703 μm per px were used for capturing and analyzing the data.

In vitro drug release tests

As produced nanocapsules of 13.75 mg were placed into 9.2 ml of 0.01 M phosphate buffer saline (PBS) in centrifuge tubes and preserved in an incubator at 37 °C to allow the nanocapsules to release drugs in PBS media. The PBS media did not contain any serum. 100 μL of PBS solution were collected from each centrifuge tubes to UV transparent 96-well plates at 24-h interval to measure the absorbance peak for each drug (paclitaxel and GW 2580)

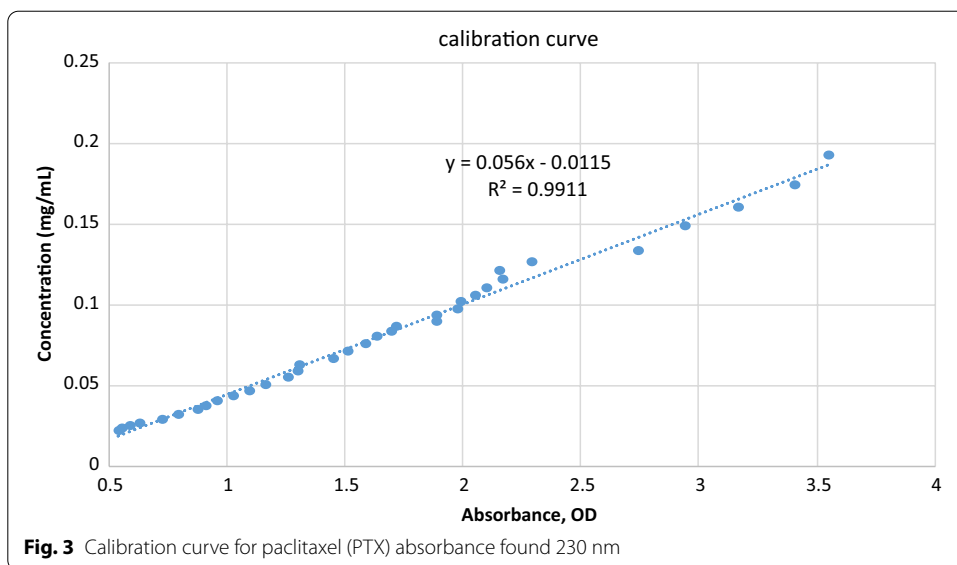


Fig. 3 Calibration curve for paclitaxel (PTX) absorbance found 230 nm

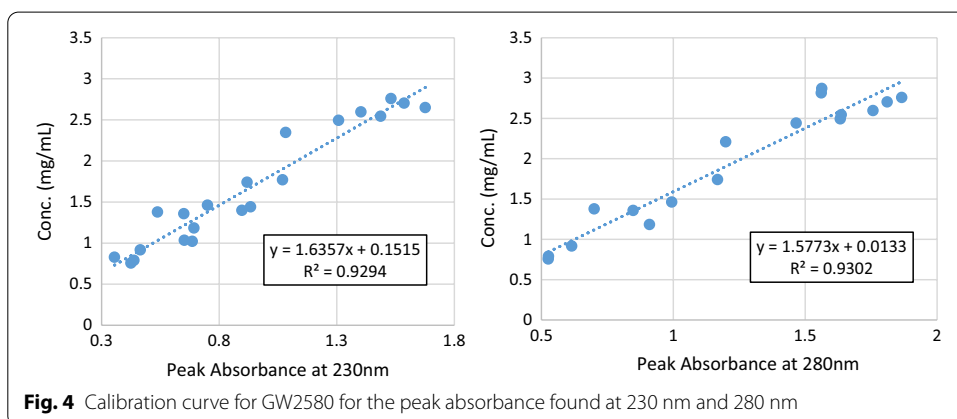


Fig. 4 Calibration curve for GW2580 for the peak absorbance found at 230 nm and 280 nm

from which the amount of released drug from nanocapsules within that time was found. Calibration curves for paclitaxel and GW2580 were plotted based on the absorbance and the corresponding drug concentrations for respective drugs. The absorbance of drug is proportional to their concentration in PBS solution. Calibration curves for paclitaxel and GW2580 were plotted individually based on the absorbance and the corresponding known drug concentrations for respective drugs. Figures 3 and 4 show the calibration curves for paclitaxel and GW2580 drugs, respectively. GW2580 has two distinct absorbance peaks near 230 nm and 280 nm wavelength, respectively. A correlation between these two absorbances was established experimental calibration curves as follows:

$$\begin{aligned}
 \text{GW2580 concentration} : 1.6357 * \text{Abs}_{230} + 0.1515 &= 1.5773 * \text{Abs}_{280} + 0.0133 \\
 \Rightarrow \text{Abs}_{230} &= 0.964 * \text{Abs}_{280} - 0.084
 \end{aligned}
 \tag{1}$$

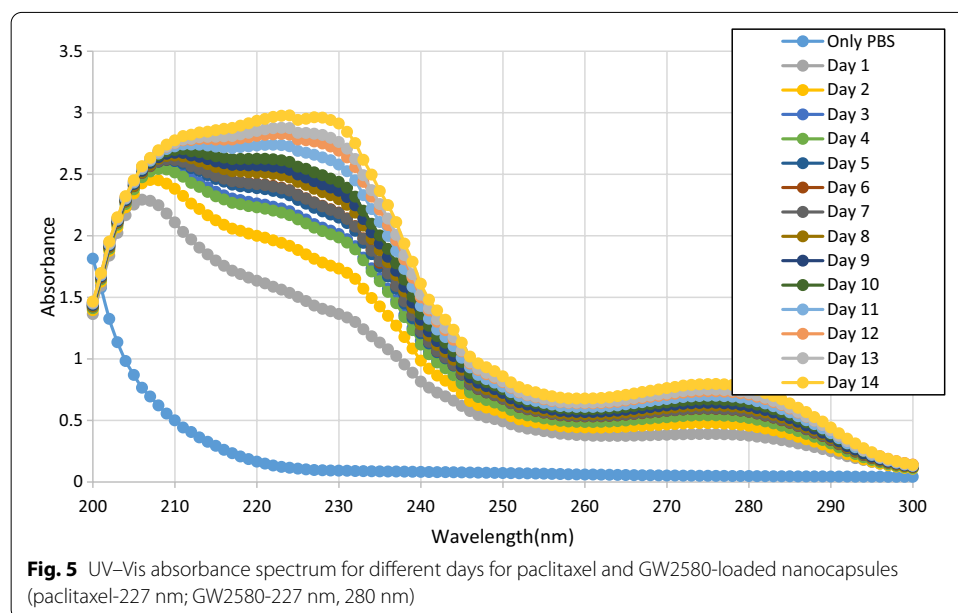
where Abs_{230} = local absorbance at 230 nm wavelength; Abs_{280} = local absorbance at 280 nm wavelength.

A vortex mixer was used to make the solution homogenized before taking samples. Samples' absorbance was measured using a UV-Vis spectrometer. Paclitaxel (PTX) has a maximum absorbance at 230 nm and GW2580 has a maximum absorbance at 230 nm and 280 nm. At 230 nm, both the drugs (PTX and GW2580) showed a peak absorbance. Therefore, the absorbance spectrum at 230 nm is a combined absorbance for both drugs, which is illustrated in Fig. 5. From the absorbance spectrum for multidrug-loaded nanocapsules the absorbance at 280 nm represents the amount of GW2580 releasing from nanocapsules in PBS media. Hence, the concentration of GW2580 was first calculated based on the absorbance at 280 nm. The absorbance of GW2580 at 230 nm was found from the calibration curve of GW2580 for both 230 nm and 280 nm and the correlation is shown as equation-1. Then this GW2580 absorbance is deducted from the combined absorbance found at 230 nm to get the absorbance that corresponds to paclitaxel. The calibration curves against the absorbance were used to determine the actual cumulative drug release at each day. After the 2 weeks of the release test the amount of cumulative drugs did not increase. The maximum drug released during the overall test period were measured from the cumulative total drug until the end of the test period. The percent release of the specific drug on each day was measured compared with the maximum cumulative drugs.

Pristine PCL showed minimal absorbance (less than background absorbance of only PBS) which was also found by other researchers (Jalili-Firoozinezhad et al. 2017), all absorbance came mostly from the drugs inside the capsules. We did not observe any interference of absorbance peaks with drugs and polymer PCL.

MDA MB 231 cells, culture methods, treatments, and cell viability assay

Human Triple Negative Breast Cancer (TNBC) cell line, MDA-MB-231 was cultured in high glucose-containing Dulbecco's modified Eagle medium (DMEM) supplemented with 10% fetal bovine serum, and 4.0 Mm L-glutamine (Thermo Scientific). The cells



were maintained at 37 °C in a normoxic (21% O₂) chamber. At confluency, the cells were split into 2.1×10^6 cells per T75 flask and maintained at regular growth condition until attached properly and made 70–80 confluent. The effects of drugs in nanocapsules were determined by cell viability assay. Cell viability was measured using a Cell Proliferation Reagent WST-1 (Millipore, Sigma, USA). Briefly, MDA-MB-231 cells were plated at a density of 1×10^4 cells/well in 96-well plates in 100 µL DMEM with 10% FBS. Then the cells were treated with nanocapsules containing paclitaxel at 100 mM concentration for 24 and 48 h. Control groups contained DMEM-HG media only. Thereafter, 10 µL of WST-1 solution were added to each well and the plates were incubated at 37 °C for an additional 4 h. The absorbance of each well was then measured at 490 nm using Victor3 1420 Multilabel Reader (Perkin Elmer, Waltham, MA, USA). Medium with 10% FBS was used as background and subtracted from the samples.

Raw 264.7 cells, culture methods, treatments, and cell viability assay

RAW264.7 mouse macrophage cell line was used for in vitro cytotoxicity assays using GW2580 containing nanocapsules as RAW 264.7 cells are CSF1R-positive cells. RAW264.7 were grown in DMEM media containing 10% FBS. At 80% confluence, cells were collected and replated in 96-well plates at a density of 1×10^4 cells/well in 96-well plates in 100µL DMEM with 10% FBS. Then the cells were treated with nanocapsules containing GW2580 at 100 mM concentration for 24 and 48 h. Control groups contained DMEM media only. Thereafter, 10 µL of WST-1 solution were added to each well and the plates were incubated at 37 °C for an additional 4 h. The absorbance of each well was then measured at 490 nm using Victor3 1420 Multilabel Reader (Perkin Elmer, Waltham, MA, USA). Medium with 10% FBS was used as background and subtracted from the samples. Cell viability was measured as absorbance and performed in triplicates.

Methods for in vivo treatment and survival study

All the experiments were performed according to the National Institutes of Health (NIH) guidelines and regulations. The Institutional Animal Care and Use Committee (IACUC) of Augusta University (protocol #2014–0625) approved all the experimental procedures. All animals were kept under standard barrier conditions at room temperature with exposure to light for 12 h and dark for 12 h. Food and water were offered ad libitum. Tumors were implanted orthotopically in animals with bodyweight between 20 and 22 g under ketamine (50 mg/kg)-xylazine (10 mg/kg) anesthesia (intraperitoneal injection). All animals received buprenorphine SR (1.2 mg/kg) subcutaneously to minimize post-surgical pain. The depth of anesthesia was checked by pinching skin or toe. The humane endpoint of the survival studies was the fulfillment of the criteria for euthanasia at the end of the survival studies (survival), which was by determining body weight (loss of more than 15% of baseline body weight), moribund, coma, paraplegia, inability to drink/eat. All animals were checked 2–3 times a week. None of the animals that underwent TME analysis and enrolled in survival studies died prematurely. All animals were treated with soft chow, apple, and subcutaneous fluid when they started signs of ruffled fur, loss of weight, lethargy, and dehydration. The animals were humanely euthanized once the euthanasia criteria were achieved. All efforts were made to ameliorate the suffering of

animals. CO₂ (displacement rate of 30–70% of the chamber volume with CO₂ per minute) with a secondary method (bilateral thoracotomy or collection of major organs) was used to euthanize animals for tissue collection. Death was confirmed by established criteria of lack of breathing, lack of corneal reflex, lack of response to a firm toe pinch, and rigor mortis.

Cell line

4T1, a murine mammary aggressive breast cancer cell line from a BALB/cfC3H mouse, was originally obtained from the American Type Tissue Culture Collection (ATCC), and modified by Dr. Hassan Korkaya (Augusta University) to express the luciferase gene reporter. For cell cultures and propagation, cells were grown in Roswell Park Memorial Institute 1640 medium (RPMI) (Thermo Scientific), supplemented with 10% fetal bovine serum (FBS) (Nalgene-GIBCO), 2 mM glutamine (GIBCO, Grand Island, NY, USA) and 100 U/mL penicillin and streptomycin (GIBCO, Grand Island, NY, USA) at 5% CO₂ at 37 °C in a humidified incubator.

Tumor model

4T1 cells expressing the luciferase gene were orthotopically implanted in NSG J-1 mice (Jackson Laboratory, Main USA). All the mice were between 5 and 6 weeks of age and weighing 18–20 g. Animals were anesthetized using a mixture of xylazine (20 mg/kg) and ketamine (100 mg/kg) through intraperitoneal administration. Then the hair was removed for the right half of the abdomen by using hair removal ointment, and then the abdomen was cleaned by povidone-iodine and alcohol. A small incision was made in the middle of the abdomen, and the skin was separated from the peritoneum using blunt forceps. Separated skin was pulled to the right side to expose the mammary fat pad and 50,000 4T1 cells in 50 µL Matrigel (Corning, NY, USA) were injected. Tumor growth was monitored every week. In *in vivo*, optical images were obtained every week to keep track of primary tumor and metastasis development by injecting 100 µL of luciferin (3 mg/mL) intraperitoneally followed by the acquisition of bioluminescence signal by spectral AmiX optical imaging system (Spectral instruments imaging, Inc. Tucson, AZ). The photon intensity/mm/sec was determined by Ami-view software (version 1.6.0). The animals were anesthetized using an isoflurane vaporizer chamber (2.5% Iso: 2 ± 3 L/min O₂) and maintained under anesthesia (2% with oxygen) during the procedure.

Nanonized combined Paclitaxel and GW2580 encased in PCL sheath were collected from the Petri dishes by using a sterile scraper and weighed. The percentage of paclitaxel and GW2580 was approximately 2.7% and 22.2%, respectively, in the combined drug formulations, sterile water was added to the formulation followed by sonication to make an injectable solution. Drug formulation was administered into the tumor-bearing mice intravenously through the tail vein in 100 µL solution at a dose of 20 mg/kg/day for paclitaxel or 160 mg/kg/day for GW2580. Treatment was started on day 8 post-implantation and continue for 2 weeks (every alternate day, a total of 6 doses).

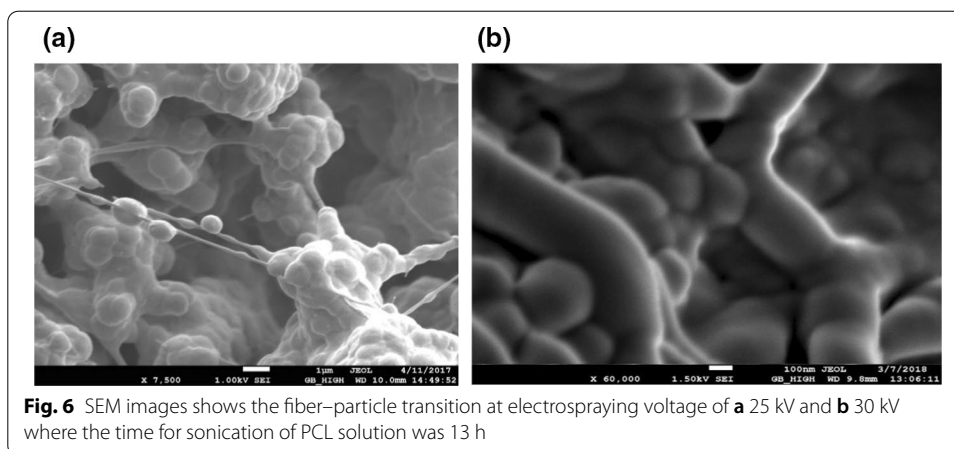


Fig. 6 SEM images shows the fiber–particle transition at electro spraying voltage of **a** 25 kV and **b** 30 kV where the time for sonication of PCL solution was 13 h

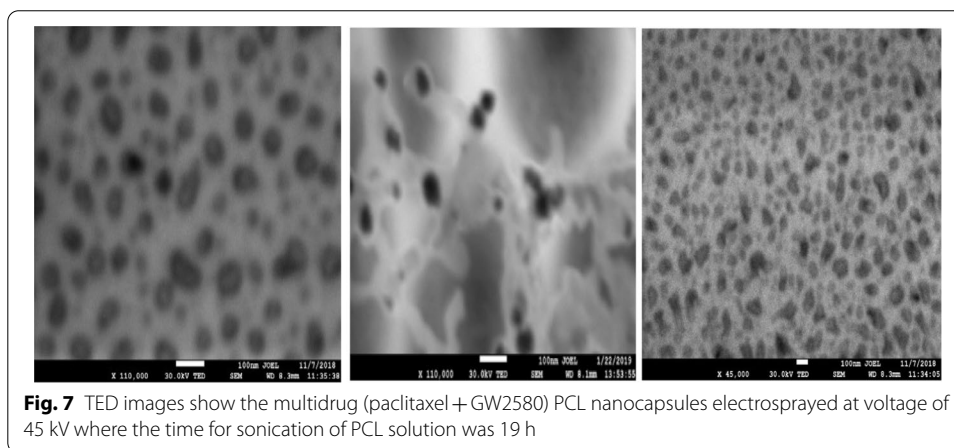


Fig. 7 TED images show the multidrug (paclitaxel + GW2580) PCL nanocapsules electro sprayed at voltage of 45 kV where the time for sonication of PCL solution was 19 h

Results and discussion

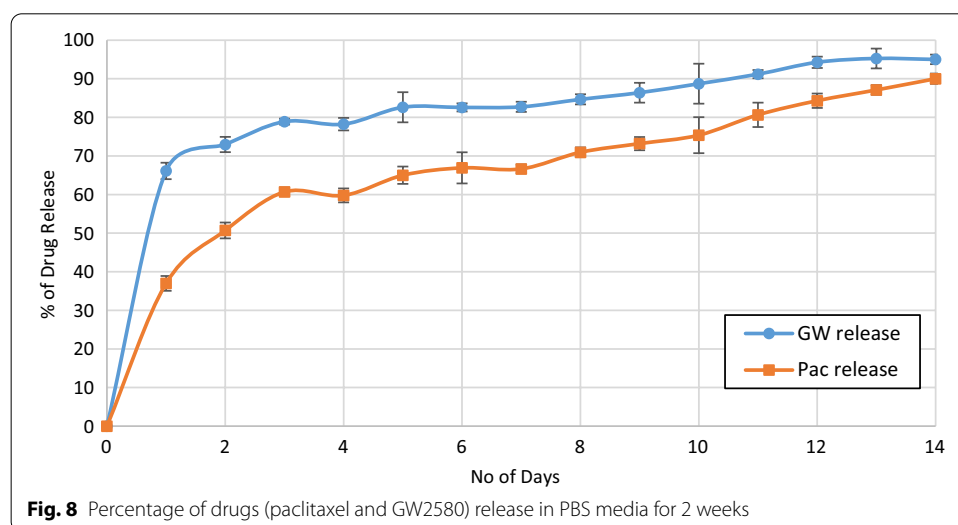
Figure 6 shows the SEM images of fiber particle transition phases electro sprayed at a voltage between 25 and 30 kV. Energy Dispersive X-ray showed no presence of drugs at the outer surface indicates the encapsulation of both the drugs. Samples were electro sprayed with a voltage between 40 and 45 kV directly on TEM grids made of lacey carbon copper. PCL was sonicated for a longer period (19 h) in this case before the electro spraying of the nanocapsules.

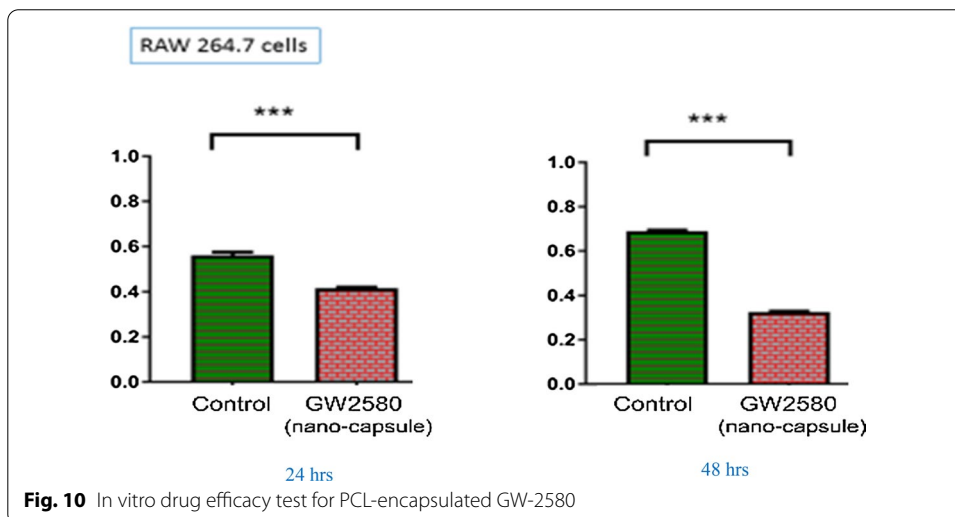
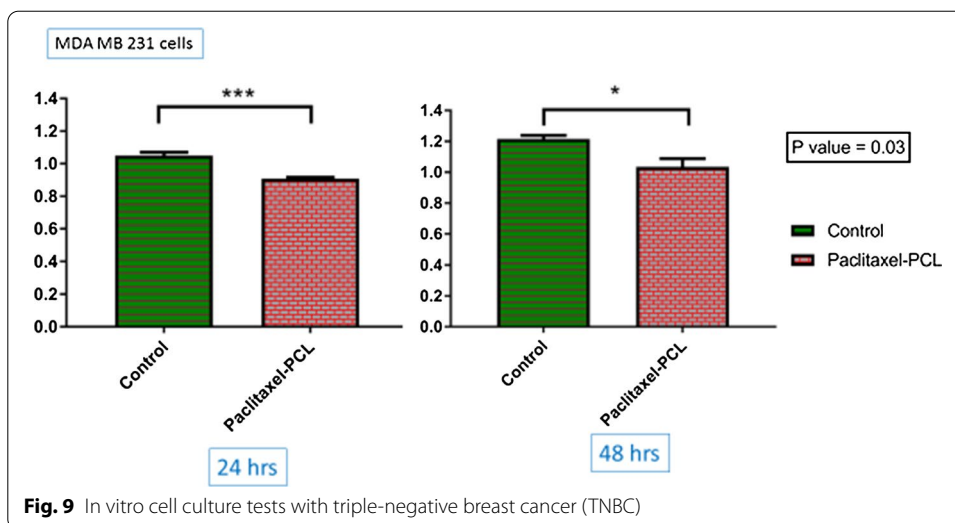
TEM image, shown in Fig. 7, was analyzed using ImageJ (Version 1.53i) software to estimate the particle size distribution. The particles in the image were found within 20–100 nm size range. No drug compounds were detected by the EDS at the outer surface. The observation is also consistent with the release test since no pattern of burst release was observed during the drug release test. As can be seen in Fig. 4, the size distribution of the produced nanoparticles is less than 100 nm even before the osmosis filtering. The total drugs (paclitaxel + GW2580) in the core was about 25% and the rest was the sheath biopolymer PCL. All these injectable nanocapsules were produced using electro spraying techniques with the innovative feeding and spinneret system as shown in Fig. 2.

The distribution of particle sizes as well as the zeta potential of the nanocapsules containing both drugs was consistent in two different samples. It is to note that the nanocapsules tend to agglomerate quickly and become larger particles if not dispersed using ultrasonic forces. The measured particle size was 168.95 ± 60.5 nm. The measured zeta potential was -21.57 ± 0.17 mV at 25°C .

As can be seen in Fig. 8 for the combined drug nanocapsules, the drug release profile is slowly sustainable for prolonged release. No burst release of the drugs was observed. Approximately 60–70% of drugs were released within the first 2–4 days, however, the rest of the drugs were released over the next 12 days. It indicates a prolonged and sustainable release pattern of the drugs from the nanocapsules. It is also observed that the release of paclitaxel is slightly slower compared to the release of GW-2580 initially, which is predictable due to the higher percentage of GW2580. In our previous study (Sakib et al. 2017) of encapsulated 5-fluorouracil (FU) and paclitaxel into biocompatible polycaprolactone (PCL) nanofibers (NFs) using core-sheath electrospinning process, encapsulated NFs demonstrated consistent drug release pattern for 25 days in PBS media and increased cytotoxicity in comparison to pristine drug when tested in human prostatic cancer and breast cancer cells. The encapsulation efficiency of the drug-loaded nanofibers was 77.5% and the amount of drug was only 4–5% of sheath polymer.

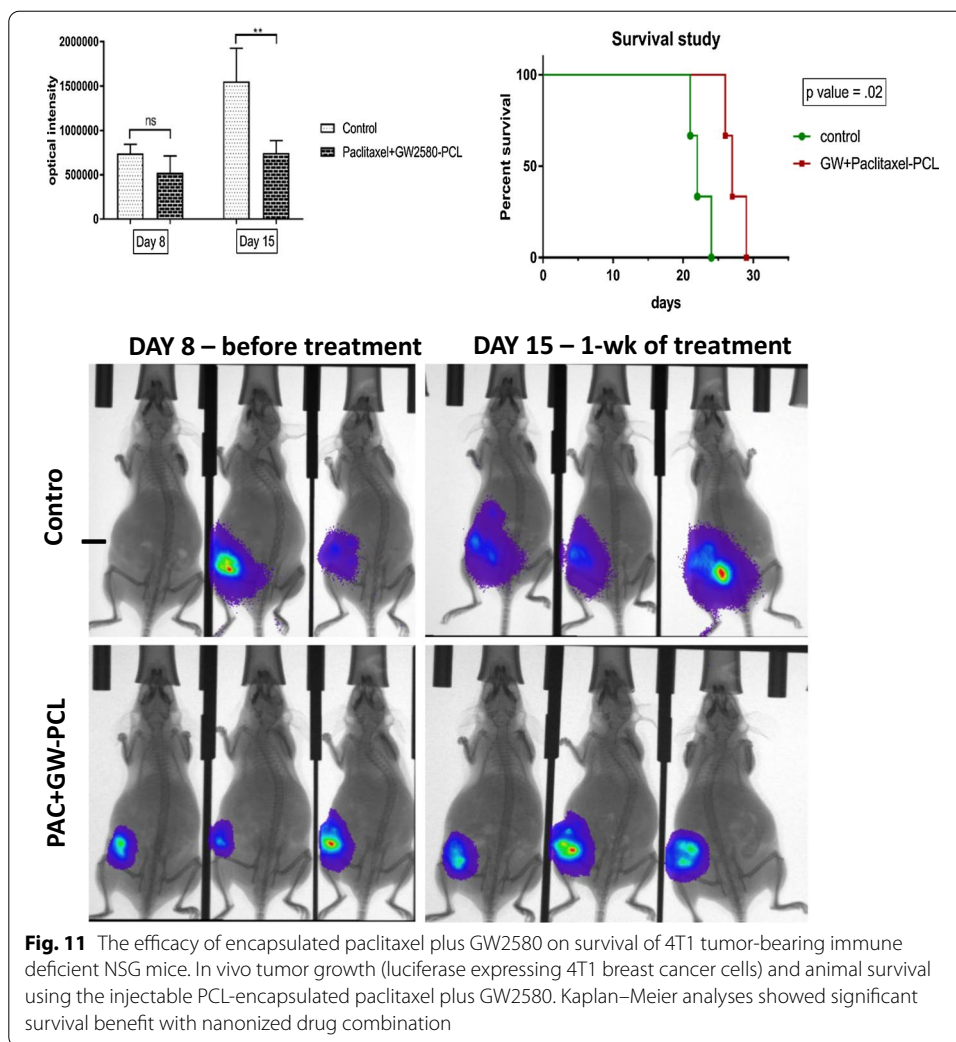
Cell viability which was measured as absorbance and was performed in triplicates. A decrease in cell proliferation was observed following the addition of nanocapsules containing paclitaxel in both 24 h and 48 h as shown in Fig. 9. Similar phenomena were observed with cancer drug-loaded PCL nanofibers (Sakib et al. 2017). Cell viability was determined by WST assay and trypan blue dye exclusion test. In both assays, PCL containing paclitaxel, 5-FU (fluorouracil) and both Paclitaxel and 5-FU decreased cell viability between 33 and 50%. However, nanofibers are not injectable due to its length scale. Also, a significant decrease in cell proliferation was observed following the addition of nanocapsules containing GW2580 in both 24 h and 48 h (Fig. 10). The *in vitro* results showed the effectiveness of the encapsulated individual drugs. Encapsulated Paclitaxel decreased the viability of breast cancer cells similar to that of naked paclitaxel mediated





cells killing as shown previously (Liebmann et al. 1993). GW2580 is a CSF1R antagonist and its effects will only be seen in cells that express CSF1R such as myeloid cells. We proved the effectiveness of encapsulated GW2580 by using RAW264.7 cells, which are mouse macrophages and express abundant CSF1R (Menke et al. 2009; Barbetti et al. 2014). The results indicate that encapsulation does not alter the function of the nanonized drugs.

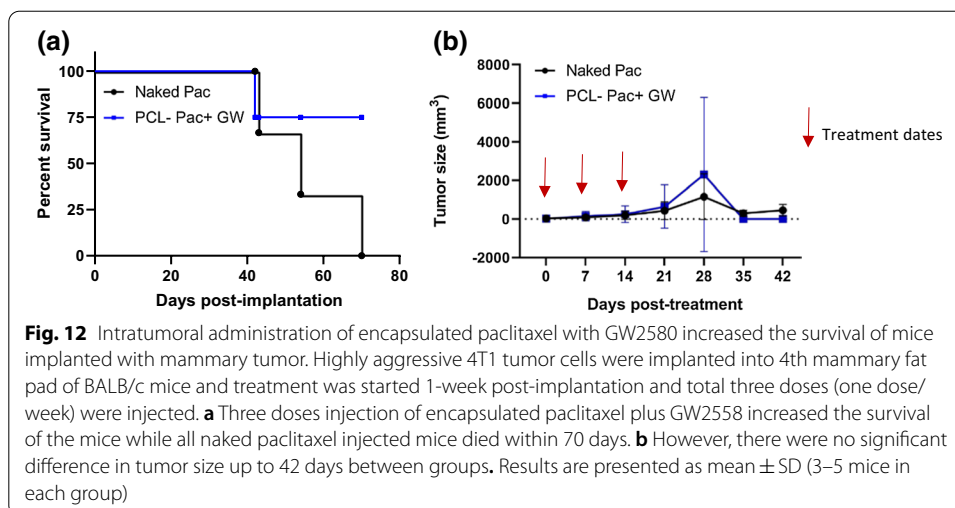
It has been observed that all animals tolerated the nanonized combined paclitaxel and GW2580. There were no adverse effects, with respect to weight loss, movement, and other well-being, observed during the therapy. All control animals died within 24 days, but the animals that received treatments survived for 29 days as shown in Fig. 11. Kaplan–Meier statistical analysis showed a significant survival benefit with the combination of nanonized paclitaxel and GW2580. While the optical density of the tumor on day 8 post-implantation for all the animals (both groups) did not show any significant



difference, on day 15 (after 1 week of treatment) group of animals injected with nanonized combined paclitaxel and GW2580 showed a significant reduction of optical intensity.

To investigate the efficacy of nanoscale encapsulation of cancer drugs CSF-1R inhibitor (GW2580) and Paclitaxel into biocompatible polycaprolactone (PCL) nanocapsules in tumor growth and metastatic outgrowth, we utilized the metastatic 4T1 tumor cells. Murine 4T1 cells were originally isolated from a spontaneous mammary tumor in the BALB/c strain and have been reported to show characteristics of the human triple-negative breast cancer (TNBC) subtype. We previously showed that 4T1 tumor cells disseminate into distant organs as early as 1-week post-implantation (Borin et al. 2016; Piranlioglu et al. 2019) and cause the death of mice within 8 weeks (Ouzounova et al. 2017). To determine its effect of the encapsulated drug and naked paclitaxel, we first implanted 50,000 4T1 tumor cells into the mammary fat pad of syngeneic mice and started treatment (**intratumor**) 1-week post-implantation.

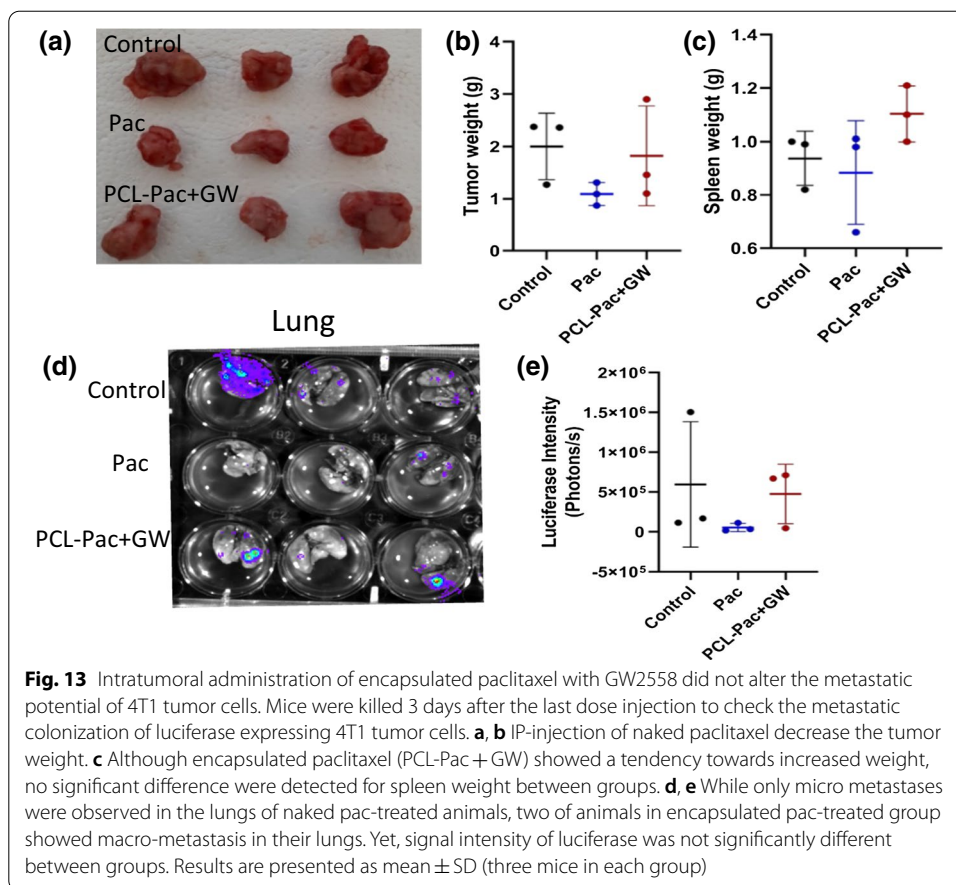
After three doses of injection (one dose/week), the treatment was terminated, and mice were followed for tumor growth and survival. In the first set of mice, only one



mouse in the encapsulated group died within 40 days and the remaining mice were tumor-free after treatment and survived until the time we followed up. However, all the mice in the naked paclitaxel-treated group deceased within 70 days (Fig. 12a, b) which is longer than the tumor-bearing mice without any treatment. Next, we examine the efficacy of encapsulated paclitaxel and GW2580 on the metastatic outgrowth of disseminated tumor cells. GW2580 is a selective inhibitor of colony-stimulating factor 1-receptor (CSF1R), which is a key regulator of myeloid cell proliferation, survival, and differentiation (Hume and MacDonald 2012). Inhibition of CSF1R has been shown to alter the recruitment and polarization of immunosuppressive myeloid cells (Stafford et al. 2016). Our group also showed that pre-treatment of mice with CSF1R inhibitor, GW2580 before tumor implantation prevent the recruitment of myeloid cell infiltration into lung, one of the main metastasis-targeting organ for breast cancer cells (Borin et al. 2017). The second set of mice euthanized to examine metastatic colonization of tumor cells in the lungs 72 h after the last injection. IP-injection of naked paclitaxel decreased the tumor weight but this decrease was not significant compared to control or encapsulated treatment (Fig. 13a, b). Although encapsulated pac (PCL-Pac + GW intra-tumoral administration) showed a tendency towards increased weight, no significant difference was detected for the weight of spleens between groups (Fig. 13c). Next, we performed ex vivo lung imaging and it showed that micrometastatic colonization of tumor cells in the lungs of naked pac-treated animals whereas two of animals in the encapsulated pac-treated group showed macro-metastasis in the same organ. Yet, the signal intensity of luciferase was not significantly different between groups (Fig. 13d, e).

Conclusions

Multicancer (paclitaxel + GW2580) drug nanocapsules were produced using a coaxial electrospinning technique. Nanonized multi-cancer drugs were encapsulated in a PCL shell. The drug doses ratio and the polymer-to-drug ratio were controlled by engineered process parameters. The produced nanocapsules were less than 100 nm in size and showed prolonged and sustained drug release for both the drugs. In vivo results proved our hypothesis that nanocapsules containing multiple drugs will accumulate and release



the drugs to cause sustained effects on the tumor growth and increase survival due to the effect on both tumor cells (by Pac) and myeloid cells (by GW2580). Our results prove the effects of the nanocapsules containing Pac + GW2580 when administered IV and local administration to enhance survival, although metastatic potential has not been altered. The effects might be due to increased accumulation (for EPR effects) and sustained release for the PCL-based capsule. The studies showed the importance of making nanocapsules containing nanocrystals of multiple drugs, which will pave the way of making multiple drug combinations in a controlled manner and capsules can be designed for sustained release of the drugs after accumulation into the TME. TME-directed therapy can be a norm in future cancer treatment strategies.

Abbreviations

PCL: Polycaprolactam; CSF1R: Colony-stimulating factor 1 receptor; CNTs: Carbon nanotubes; QD: Quantum dots; TME: Tumor microenvironment; SEM: Scanning electron microscope; TED: Transmission electron detector; IACUC: Institutional Animal Care and Use Committee; NSG: NOD SCID gamma; PBS: Phosphate buffer saline; DMEM: Dulbecco's modified Eagle medium; TNBC: Triple-negative breast cancer.

Acknowledgements

The authors would like to acknowledge support from the National Science Foundation (NSF). The MRI (Grant #DMR-1337545) equipment was used in the experimental study and Georgia Southern University faculty research seed grant. The authors would also like to acknowledge MRK0 and Georgia Cancer Center Start-up fund (ASA).

Authors' contributions

Dr. MK is the Principal Investigator. Dr. MK has planned and designed the experiments for processing the nanocapsules, release tests and all imaging and morphology analysis. He has prepared the manuscript. Dr. AA is the main collaborator and co-investigator for the study. Dr. AA has designed facilitated and supervise the in vivo and in vitro studies and interpreted the results. MMH was the graduate student who worked in the research project under the supervision of Dr. MK. He performed the fabrication and processing of the nanocapsules and released tests acquire the data/experimental observations and record the findings. AB is the undergraduate student who worked in the project and contributed to optimize materials processing and characterization under the supervision of Dr. MK. RP, a post-doctoral fellow who conducted and collected results for the in vivo studies. MR was a graduate (PhD) student who have contributed the in vitro studies and drug doses combinations. AA, a post-doctoral fellow measured the particle size and zeta potential. RP, AA, and MR worked in the project under the supervision of Dr. AA and conducted and contributed to in vivo and in vitro studies, data/results analysis. All authors read and approved the final manuscript.

Funding

Not applicable.

Availability of data and materials

All data generated or analyzed during this study are included in this submitted article. Data/experimental results are presented in the manuscript and if appropriate, datasets/experimental results used and/or analyzed during the current study are available from the corresponding author on reasonable request.

Declarations

Ethics approval and consent to participate

All the in vivo experiments were performed according to the National Institutes of Health (NIH) guidelines and regulations. The Institutional Animal Care and Use Committee (IACUC) of Augusta University (protocol #2014–0625) approved all the experimental procedures. Ethics statement has been provided in the manuscript in the in vivo study section.

Consent for publication

We would like to mention that this manuscript has not been published and or not submitted elsewhere for publication while being considered by the journal *Cancer Nanotechnology*.

Competing interests

The authors declare that they have no competing interests.

Author details

¹Department of Mechanical Engineering, Georgia Southern University, Statesboro, GA 30458, USA. ²Georgia Cancer Research Center, Augusta University, Augusta, GA 30912, USA.

Received: 3 May 2021 Accepted: 2 February 2022

Published online: 22 February 2022

References

- Ajuffali IA, Mock NJ, Costyn JL, Nguyen H, Nagy T, Cummings SB, Arnold DR (2011) Enhanced antitumor activity of low-dose continuous administration schedules of topotecan in prostate cancer. *Cancer Biol Ther* 12(5):407–420
- Barbetti V, Morandi A, Tusa I, Digiacomio G, Rivero M, Marzi I, Cipolleschi MG, Bessi S, Giannini A, Di Leo A, Dello Sbarba P, Rovida E (2014) Chromatin-associated CSF-1R binds to the promoter of proliferation-related genes in breast cancer cells. *Oncogene* 33:4359–4364. <https://doi.org/10.1038/onc.2013.542>
- Borin TF, Arbab SA, Gelaleti GB, Ferreira CL, Moschetta GM, Perassi JVB, Iskandar ASM, Varma NRS, Shankar A, Coimbra BV, Fabri Oliveira AV, Zuccari CPAD (2016) Melatonin decreases breast cancer metastasis by modulating Rho-associated kinase protein-1 expression. *J Pineal Res* 60(1):3–15. <https://doi.org/10.1111/jpi.12270>
- Borin TF et al (2017) CSF-1R inhibitor prevented pre-metastatic lung niches in metastatic mammary tumor. *Can Res*. <https://doi.org/10.1158/1538-7445.AM2017-1043>
- Butowski N, Colman H, De Groot JF, Omuro AM, Nayak L, Wen PY (2015) Orally administered colony stimulating factor 1 receptor inhibitor PLX3397 in recurrent glioblastoma: an ivy foundation early phase clinical trials consortium phase II study. *Neuro Oncol* 18(4):557–564. <https://doi.org/10.1093/neuonc/nov245>
- Chen Z, Zhang A, Wang X et al (2017) The advances of carbon nanotubes in cancer diagnostics and therapeutics. *J Nanomater*. <https://doi.org/10.1155/2017/3418932>
- Conde J, Dias JT, Graú V, Moros M, Baptista PV, Fuente JM (2014) Revisiting 30 years of biofunctionalization and surface chemistry of inorganic nanoparticles for nanomedicine. *Front Chem* 2:48
- Eatemadi A, Daraee H, Karimkhanloo H et al (2014) Carbon nanotubes: properties, synthesis, purification, and medical applications. *Nanoscale Res Lett* 9(1):393
- Fang F et al (2013) Mitochondrial modulation of apoptosis induced by low-dose radiation in mouse testicular cells. *Biomed Environ Sci* 26(10):820–830
- Ghosh P, Han G, De M, Kim C, Rotello V (2008) Gold nanoparticles in delivery applications. *Adv Drug Deliv Rev* 60(11):1307–1315
- Greish K (2010) Enhanced permeability and retention (EPR) effect for anticancer nanomedicine drug targeting. *Cancer Nanotechnol* 625:25–37. https://doi.org/10.1007/978-1-60761-609-2_3

- Hume DA, MacDonald KP (2012) Therapeutic applications of macrophage colony stimulating factor-1 (CSF-1) and antagonists of CSF-1 receptor (CSF-1R) signaling. *Blood* 119(8):1810–1820
- Iyer AK, Khaled G, Fang J, Maeda H (2006) Exploiting the enhanced permeability and retention effect for tumor targeting. *Drug Discov Today* 11(17):812–818
- Jalili-Firooznezhad S, Moghadam MHM, Ghanian MH, Ashtiani MK, Alimadadi H, Baharvand H, Scherberich A (2017) Polycaprolactone-templated reduced-graphene oxide liquid crystal nanofibers towards biomedical applications. *RSC Adv* 7(63):39628–39634
- Kummari, Alfred R (2018) Emulsion based processing of drug loaded particles for targeted drug delivery. Electronic Theses and Dissertations. 1869. <https://digitalcommons.georgiasouthern.edu/etd/1869>
- Li Z, Wang C (2013) In one-dimensional nanostructures—electrospinning technique and unique nanofibers. Springer, Berlin, pp 15–28
- Liebmann J, Cook J, Lipschultz C, Teague D, Fisher J, Mitchell J (1993) Cytotoxic studies of paclitaxel (Taxol®) in human tumour cell lines. *Br J Cancer* 1993(68):1104–1109. <https://doi.org/10.1038/bjc.1993.488>
- Menke J, Iwata Y, Rabacal WA, Basu R, Yeung YG, Humphreys BD, Wada T, Schwarting A, Stanley ER, Kelley VR (2009) CSF-1 signals directly to renal tubular epithelial cells to mediate repair in mice. *J Clin Invest* 119:2330–2342. <https://doi.org/10.1172/jci39087>
- Mosqueira VC, Legrand P, Gulik A, Gref OBR, Labarre D, Barratt G (2001) Relationship between complement activation, cellular uptake and surface physicochemical aspects of novel peg modified nanocapsules. *Biomaterials* 22(22):2967–2979
- Ouzounova M et al (2017) Monocytic and granulocytic myeloid derived suppressor cells differentially regulate spatiotemporal tumour plasticity during metastatic cascade. *Nat Commun* 8:14979
- Patwardhan PP, Surriga O, Beckman MJ, Stanchina E, Dematteo RP, Tap WD (2014) Sustained inhibition of receptor tyrosine kinases and macrophage depletion b PLX3397 and rapamycin as a potential new approach for the treatment of MPNSTs. *Clin Cancer Res* 20:3146–3158
- Piranlioglu R et al (2019) Primary tumor-induced immunity eradicates disseminated tumor cells in syngeneic mouse model. *Nat Commun* 10(1):1430
- Prabhakar U, Maeda H, Jain RK, Sevick EM, Zamboni W, Farokhzad OC, Barry ST, Gabizon A, Grodzinski P, Blakey DC (2013) Challenges and key considerations of the enhanced permeability and retention effect for nanomedicine drug delivery in oncology. *Cancer Res* 73(8):2412–2417
- Probst CE, Zrazhevskiy P, Bagalkot V, Gao X (2013) Quantum dots as a platform for nanoparticle drug delivery vehicle design. *Adv Drug Deliv Rev* 65(5):703–718
- Sakib I, Mohammad R, Ali S, A, M Khan. (2017) Encapsulation of anticancer drugs (5-fluorouracil and paclitaxel) into polycaprolactone (PCL) nanofibers and in vitro testing for sustained and targeted therapy. *J Biomed Nanotechnol* 13:1–12
- Sercombe L et al (2015) Advances and challenges of liposome assisted drug delivery. *Front Pharmacol*. <https://doi.org/10.3389/fphar.2015.00286>
- Shi J, Kantoff PW, Wooster R, Farokhzad OC (2017) Cancer nanomedicine: progress, challenges and opportunities. *Nat Rev Cancer* 17(1):20–37. <https://doi.org/10.1038/nrc.2016.108>
- Smith CC, Zhang C, Lin KC, Lasater EA, Zhang Y, Massi E (2015) Characterizing and overriding the structural mechanism of the quizartinib-resistant FLT3 “gatekeeper” F691L mutation with PLX3397. *Cancer Discov* 5:668–679
- Stafford JH et al (2016) Colony stimulating factor 1 receptor inhibition delays recurrence of glioblastoma after radiation by altering myeloid cell recruitment and polarization. *Neuro Oncol* 18(6):797–806
- Sun T, Zhang YS, Pang B, Hyun DC, Yang M, Xia Y (2014) Engineered nanoparticles for drug delivery in cancer therapy. *Angew Chem Int Ed* 53(46):12320–12364
- Upreti M, Jyoti A, Sethi P (2013) Tumor microenvironment and nanotherapeutics. *Transl Cancer Res* 2(4):309–319
- Voura EB, Jaiswal JK, Mattoussi H, Simon SM (2004) Tracking metastatic tumor cell extravasation with quantum dot nanocrystals and fluorescence emission-scanning microscopy. *Nat Med* 10(9):993–998
- Wahajuddin, Arora S (2012) Superparamagnetic iron oxide nanoparticles: magnetic nanoplatforms as drug carriers. *Int J Nanomed* 7:3445–3471. <https://doi.org/10.2147/IJN.S30320>
- Woodruff MA, Hutmacher DW (2010) The return of a forgotten polymer—polycaprolactone in the 21st century. *Prog Polym Sci* 35:1217–1256
- Xu J, Luft JC, Yi X, Tian S, Owens G, Wang J et al (2013) RNA replicon delivery via lipid-complexed PRINT protein particles. *Mol Pharm*. <https://doi.org/10.1021/mp400190z>
- Yadav D et al (2017) Liposomes for drug delivery. *J Biotechnol Biomater*. <https://doi.org/10.4172/2155-952X.1000276>

Publisher's Note

Springer Nature remains neutral with regard to jurisdictional claims in published maps and institutional affiliations.